

Space-Time Block Codes over the Stiefel Manifold

Mohammad T. Hussien[§], Karim G. Seddik[†], Ramy H. Gohary[‡], Mohammad Shaqfeh*,
Hussein Alnuweiri*, and Halim Yanikomeroglu[‡]

[§]Department of Electrical Engineering, Alexandria University, Egypt

[†]Electronics Engineering Department, American University in Cairo, AUC Avenue, New Cairo 11835, Egypt

[‡]Department of Systems and Computer Engineering, Carleton University, Ottawa, Canada

*Department of Electrical Engineering, Texas A&M University in Qatar, Doha, Qatar

Abstract—In this paper we develop two approaches for designing unitarily-constrained space-time block codes, which are suitable for communicating high-resolution information in layered multiple-input multiple-output broadcast channels. Unlike existing space-time codes, which are usually synthesized from standard phase-shift keying (PSK) or quadrature amplitude modulation constellations, the space-time codes proposed herein are designed using direct optimization over the unitary group. In comparison with conventional unitary space-time block codes, including Alamouti code with PSK constellations, the space-time codes generated by the proposed approaches exhibit significantly better performance, more favorable distance spectra and more effective utilization of the degrees of freedom that underlie the unitary group.

I. INTRODUCTION

In multi-resolution broadcast communication systems two classes of receivers can be identified: low-resolution (LR) receivers, which do not have access to channel state information (CSI) and can only perform non-coherent detection and high-resolution (HR) receivers, which have access to reliable CSI and can perform coherent detection [1]. The LR information constitutes the basic information that must be reliably communicated to both classes of receivers, whereas the HR information constitutes the incremental information that only the HR receivers have access to.

Related work that considers transmitting coherent and non-coherent data in a multiuser MIMO (MU-MIMO) settings appears in [2] and [3]. The focus therein is on deriving the achievable degrees of freedom, where our focus herein is on the design of practical unitarily-constrained space-time codes for multilayer (multi-resolution) broadcasting scenarios.

For multiple-input multiple-output systems operating at high signal-to-noise ratios (SNRs), the LR information can be reliably communicated using constellations designed on the so-called Grassmann manifold, that is, the set of tall unitary matrices that span distinct subspaces. Using this type of signaling achieves the capacity of the non-coherent MIMO channel of the LR receiver [4]. Grassmannian constellations are unitarily-invariant. In other words, the subspace spanned

by a tall unitary matrix is unaffected when this matrix is right multiplied with a square matrix. This implies that, to communicate incremental information to the HR receivers without compromising the reliability with which the basic information is received by the LR receivers, the incremental information must be encoded using square unitary matrices. Such matrices represent elements of the unitary group and their geometric role is to rotate and scale the bases of the subspace spanned by the tall unitary matrix. The Cartesian product of the tall Grassmannian matrices and the square unitary matrices gives rise to an HR constellation on the so-called Stiefel manifold, which will be discussed in the next section. The HR information conveyed by the constellation on the Stiefel manifold can only be detected coherently by the HR receivers, whereas the LR information conveyed by the constellation on the Grassmann manifold can be detected by both receivers.

Various techniques are available designing space-time Grassmannian constellations, see e.g., [5], [6]. However, techniques for designing codes on the unitary group are generally scarce. In fact, the only available designs for unitarily-constrained constellation are those in which the codes are synthesized from standard scalar phase-shift keying (PSK) and quadrature amplitude modulation constellations, e.g., Alamouti codes with PSK. In addition to being overly restrictive, codes that are synthesized in this way are not available for arbitrary square dimensions. For instance, unitary 3×3 codes are not available. To overcome this difficulty, in this paper we focus on developing two techniques for designing unitarily-constrained square space-time block codes directly on the group of square unitary matrices. The philosophy of these techniques resembles to some extent that used in [5] for generating Grassmannian constellations with maximized minimum distance between any two points. However, the main difference herein is that the design space is the unitary group rather than the Grassmann manifold. This difference results in a design objective that is fundamentally different from the one used in the case of Grassmannian constellations. In particular, herein the design objective is to maximize the minimum Euclidean distance, whereas the design objective in [5] is to maximize the chordal Frobenius norm.

In the first design approach, the points of the constellation are designed sequentially, thereby giving rise to a greedy-like technique. In contrast, in the second approach the points are

*The work of the first, second, fourth and fifth authors is supported by NPRP grant # 05-401-2-161 from the Qatar National Research Fund (a member of Qatar Foundation). The work of the third and sixth authors is supported in part by Huawei Canada Co., Ltd., and in part by the Ontario Ministry of Economic Development and Innovations ORF-RE (Ontario Research Fund - Research Excellence) program.

designed jointly. Hence, the second approach yields constellations with more favorable properties but with higher design complexity. In comparison with conventional “unitarily-constrained” space-time block codes, the ones generated by the proposed approaches possess more favorable distance spectra and subsequently better performance. It might be worth noting, that the codes generated by the proposed approaches outperform unconstrained space-time codes over a wide SNR range.

II. PRELIMINARIES

In this section we will provide a brief background on the Stiefel and Grassmann manifolds, which will be necessary for subsequent analysis.

For $T \geq M$, the Stiefel manifold $\mathbb{S}_{T,M}(\mathbb{C})$ is defined as the set of all unitary $T \times M$ matrices, that is,

$$\mathbb{S}_{T,M}(\mathbb{C}) = \{\mathbf{Q} \in \mathbb{C}^{T \times M} : \mathbf{Q}^H \mathbf{Q} = \mathbf{I}_M\}. \quad (1)$$

The Stiefel manifold $\mathbb{S}_{T,M}(\mathbb{C})$ is submanifold of $\mathbb{C}^{T \times M}$ of $TM - M^2/2$ complex dimensions.

The Grassmann manifold $\mathbb{G}_{T,M}(\mathbb{C})$ is defined as the quotient space of $\mathbb{S}_{T,M}(\mathbb{C})$ with respect to the equivalence relation that renders two elements $\mathbf{P}, \mathbf{Q} \in \mathbb{S}_{T,M}(\mathbb{C})$ equivalent if their T -dimensional column vectors span the same subspace, i.e.,

$$\mathbf{P} = \mathbf{Q}\mathbf{V}, \quad (2)$$

for some matrix \mathbf{V} in the unitary group $\mathbb{U}_M = \mathbb{S}_{M,M}(\mathbb{C})$.

Since each element of $\mathbb{G}_{T,M}(\mathbb{C})$ represents an equivalence class in $\mathbb{S}_{T,M}(\mathbb{C})$, the number of complex dimensions of the Grassmann manifold can be expressed as:

$$\begin{aligned} \dim(\mathbb{G}_{T,M}(\mathbb{C})) &= \dim(\mathbb{S}_{T,M}(\mathbb{C})) - \dim(\mathbb{S}_{M,M}(\mathbb{C})) \\ &= M(T - M). \end{aligned} \quad (3)$$

III. SYSTEM MODEL

We consider a broadcast MIMO communication system with M transmit antennas with two classes of receivers operating over the block Rayleigh flat-fading channel in Figure 1. The channel is assumed to be constant over T consecutive time slots. Using N_i to denote the number of receive antennas of the i -th receiver, the communication system can be modeled as

$$\begin{aligned} \mathbf{Y}_i &= \mathbf{X}\mathbf{H}_i + \mathbf{W}_i \\ &= \mathbf{U}\mathbf{A}\mathbf{H}_i + \mathbf{W}_i, \quad i = 1, 2, \dots, \end{aligned} \quad (4)$$

where \mathbf{Y}_i is the $T \times N_i$ received matrix of the i -th receiver, $\mathbf{X} = \mathbf{U}\mathbf{A}$ is the $T \times M$ transmitted matrix which contains both the LR and the HR information. When the SNR is sufficiently high, the capacity of the LR channel observed by, say, receiver 1 can be achieved if \mathbf{X} were isotropically distributed on $\mathbb{G}_{T,M}(\mathbb{C})$, provided that $N_1 \geq M$, $T \geq M + N_1$ and $M \leq \lfloor T/2 \rfloor$ [4]. For ease of exposition, these conditions will be assumed to be satisfied throughout. To realize the isotropic distribution for \mathbf{X} on $\mathbb{G}_{T,M}(\mathbb{C})$ under these conditions, in this paper, the LR information is encoded in the subspace spanned by the matrix \mathbf{U} and the HR information is encoded in the

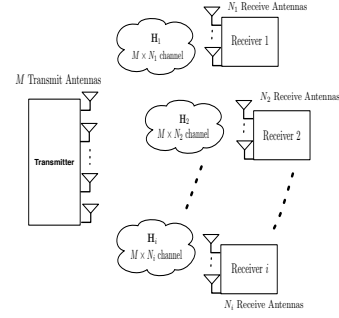


Fig. 1: The MIMO broadcast system model.

$M \times M$ unitary matrix $\mathbf{A} \in \mathbb{U}_M$, which represents a rotation of the subspace spanned by \mathbf{U} . The matrices \mathbf{H}_i and \mathbf{W}_i represent the channel and noise observed by receiver i , and the elements of these matrices are assumed to be statistically independent, identically distributed (i.i.d) circularly-symmetric zero mean complex Gaussian random variables. The entries of \mathbf{H}_i have unit variance and the entries of \mathbf{W}_i have variance N_0 . For notational convenience, we will drop the receiver index i and will allude to the coherent and non-coherent operating modes as necessary.

In our layered encoding scheme, the LR layer contains the basic information and is represented by a unitary non-coherent code, with codewords that are isotropically distributed on the complex Grassmann manifold $\mathbb{G}_{T,M}(\mathbb{C})$. Since this manifold represents the set of M -dimensional subspaces in \mathbb{C}^T , every codeword in this non-coherent code represents a particular M -dimensional subspace, which is spanned by the $T \times M$ matrix \mathbf{U} . This LR layer has the advantage that it can be decoded coherently if the receiver has reliable CSI or non-coherently if CSI is not available. In contrast, in our construction, the HR layer contains the incremental information and is represented by a coherent code with particular codewords drawn from the group of $M \times M$ complex unitary matrices \mathbb{U}_M . This layer can only be decoded coherently by a receiver that has access to reliable CSI.

IV. HR LAYER (COHERENT) CODE CONSTRUCTION

We have shown previously in [1] that restricting the matrix \mathbf{A} in (4), which represents the incremental HR information, to possess a unitary structure (drawn from the unitary group \mathbb{U}_M) ensures the preservation of the distance characteristics of the non-coherent code. With the restriction that $\mathbf{A} \in \mathbb{U}_M$ we can write $\mathbf{H} \stackrel{d}{=} \mathbf{A}\mathbf{H}$, where $\stackrel{d}{=}$ denotes equality in distribution. This implies that the performance of the LR (non-coherent) code will not be affected by the transmission of the HR information. Also, restricting the matrix \mathbf{A} to be unitary does not increase the required transmitted power, i.e., the HR (coherent) layer is completely transparent to the LR (non-coherent) layer and no additional power provisioning is required to maintain the performance of the LR layer. A candidate of such coherent codes is the standard 2×2 Alamouti scheme [7], whereby the

matrix \mathbf{A} is constructed as follows:

$$\mathbf{A} = \frac{1}{\sqrt{2}} \begin{pmatrix} s_1 & s_2 \\ -s_2^* & s_1^* \end{pmatrix}, \quad (5)$$

where s_1 and s_2 are two complex symbols drawn from any constant modulus constellation, e.g., PSK. Note that, because two symbols are transmitted in each matrix \mathbf{A} , Alamouti scheme exhausts the $M^2/2$ available degrees of freedom when $M = 2$. For larger M , coherent unitary $M \times M$ codes can be constructed directly on \mathbb{U}_M .

In this section, we design constellation points for the HR layer on the Unitary group \mathbb{U}_M where each point is represented by a unitary $M \times M$ matrix and our design criterion is to maximize the minimum Frobenius distance between these points. In our design, we use the gradient descent algorithm with curvilinear search [8], and we introduce two different approaches: the greedy approach and the direct approach.

A. The Greedy Design

In this approach, we design the constellation of $|\mathcal{C}|$ points on the Unitary Group \mathbb{U}_M in a point-by-point manner. We start by an initial point on \mathbb{U}_M , then find the next point such that it maximizes the Frobenius distance to the initial point restricting the new point to be on \mathbb{U}_M . Then, the third point is found through maximizing the minimum distance between this point and the previous two points. The operation continues till the whole constellation of $|\mathcal{C}|$ points is designed. The optimization problem for designing the i -th constellation point can be formulated as follows.

$$\mathbf{A}_i = \arg \max_{\mathbf{A}\mathbf{A}^H = \mathbf{I}} \min_{1 \leq j \leq i-1} \|\mathbf{A} - \mathbf{A}_j\|_F. \quad (6)$$

Note that maximizing the square of the Frobenius distance is equivalent to maximizing the Frobenius distance itself; therefore, the cost function in the above optimization problem can be simplified as follows.

$$\begin{aligned} \|\mathbf{A} - \mathbf{A}_j\|_F^2 &= \text{Tr} \left((\mathbf{A} - \mathbf{A}_j)^H (\mathbf{A} - \mathbf{A}_j) \right) \\ &= \text{Tr} \left(2\mathbf{I} - \mathbf{A}_j^H \mathbf{A} - \mathbf{A}^H \mathbf{A}_j \right) \\ &= 2M - 2 \text{Tr} \left(\Re \left(\mathbf{A}_j^H \mathbf{A} \right) \right). \end{aligned} \quad (7)$$

From the last equation, we can see that maximizing the minimum distance is equivalent to minimizing the maximum value of the term $\text{Tr} \left(\Re \left(\mathbf{A}_j^H \mathbf{A} \right) \right)$ where $1 \leq j \leq i-1$. Equation (6) can then be rewritten as

$$\mathbf{A}_i = \arg \min_{\mathbf{A}\mathbf{A}^H = \mathbf{I}} \max_{1 \leq j \leq i-1} \text{Tr} \left(\Re \left(\mathbf{A}_j^H \mathbf{A} \right) \right). \quad (8)$$

Define f as

$$f = \max_{1 \leq j \leq i-1} \text{Tr} \left(\Re \left(\mathbf{A}_j^H \mathbf{A} \right) \right). \quad (9)$$

Using the following approximation

$$\max_{1 \leq j \leq i-1} x_j \approx \left(\log \left(\sum_{j=1}^{i-1} e^{x_j} \right) \right)^{\frac{1}{n}}, \quad (10)$$

where n is the approximation order, the cost function f can be written as

$$\begin{aligned} f &= \max_{1 \leq j \leq i-1} \text{Tr} \left(\Re \left(\mathbf{A}_j^H \mathbf{A} \right) \right) \\ &\approx \left(\log \left(\sum_{j=1}^{i-1} e^{\text{Tr}^n \left(\Re \left(\mathbf{A}_j^H \mathbf{A} \right) \right)} \right) \right)^{\frac{1}{n}}. \end{aligned} \quad (11)$$

The design equation can then be written as follows

$$\mathbf{A}_i = \arg \min_{\mathbf{A}\mathbf{A}^H = \mathbf{I}} \left(\log \left(\sum_{j=1}^{i-1} e^{\text{Tr}^n \left(\Re \left(\mathbf{A}_j^H \mathbf{A} \right) \right)} \right) \right)^{\frac{1}{n}}. \quad (12)$$

Starting from point \mathbf{A} on the unitary group \mathbb{U}_M , it was shown in [8] that ∇f (the steepest descent direction in the tangent plane at \mathbf{A}) equals $\mathbf{S}\mathbf{A}$, i.e., $\nabla f = \mathbf{S}\mathbf{A}$, where \mathbf{S} is a skew Hermitian matrix given by $\mathbf{S} = \mathbf{G}_\mathbf{A} \mathbf{A}^H - \mathbf{A} \mathbf{G}_\mathbf{A}^H$ and $\mathbf{G}_\mathbf{A} = \frac{df}{d\mathbf{A}}$.

A trivial new point $\mathbf{Y}(\tau)$ based on ∇f would then be

$$\begin{aligned} \mathbf{Y}(\tau) &= \mathbf{A} - \tau \nabla f \\ &= \mathbf{A} - \tau \mathbf{S}\mathbf{A}, \end{aligned} \quad (13)$$

where τ is the step size.

However, the previous updating scheme does not ensure the unitarity of the new point $\mathbf{Y}(\tau)$. In order to overcome this problem, \mathbf{A} in the second term of the right hand side of (13) is replaced by $\frac{\mathbf{A} + \mathbf{Y}(\tau)}{2}$; the new point $\mathbf{Y}(\tau)$ can now be written as

$$\mathbf{Y}(\tau) = \mathbf{A} - \tau \mathbf{S} \left(\frac{\mathbf{A} + \mathbf{Y}(\tau)}{2} \right), \quad (14)$$

which can be rearranged as

$$\mathbf{Y}(\tau) = \left(\mathbf{I} + \frac{\tau}{2} \mathbf{S} \right)^{-1} \left(\mathbf{I} - \frac{\tau}{2} \mathbf{S} \right) \mathbf{A}. \quad (15)$$

This is the updating scheme that we will use in our design. Note that (15) is known as *Cayley transform*. Also note that $\mathbf{Y}(0) = \mathbf{A}$ and $\mathbf{Y}^H(\tau)\mathbf{Y}(\tau) = \mathbf{I}$ for all $\tau \in \mathbb{R}$ (i.e., $\mathbf{Y}(\tau)$ is confined to \mathbb{U}_M).

Next, we will try to derive $\mathbf{G}_\mathbf{A}$ to completely identify \mathbf{S} in (15). Equation (11) can be written as follows.

$$f \approx \left(\log \left(\sum_{j=1}^{i-1} e^{u_j} \right) \right)^{\frac{1}{n}}, \quad (16)$$

where

$$u_j = \text{Tr} \left(\Re \left(\mathbf{A}_j^H \mathbf{A} \right) \right). \quad (17)$$

Then, we have

$$\begin{aligned} \mathbf{G}_\mathbf{A} &= \frac{df}{d\mathbf{A}} \\ &= \frac{\left(\log \left(\sum_{j=1}^{i-1} e^{u_j} \right) \right)^{\frac{1}{n}-1}}{\sum_{j=1}^{i-1} e^{u_j}} \sum_{j=1}^{i-1} e^{u_j} u_j^{n-1} \frac{du_j}{d\mathbf{A}}, \end{aligned} \quad (18)$$

and

$$\frac{du_j}{d\mathbf{A}} = \mathbf{A}_j. \quad (19)$$

Substituting in (18), we get

$$\mathbf{G}_{\mathbf{A}} = \frac{\left(\log\left(\sum_{j=1}^{i-1} e^{u_j^n}\right)\right)^{\frac{1}{n}-1}}{\sum_{j=1}^{i-1} e^{u_j^n}} \sum_{j=1}^{i-1} e^{u_j^n} u_j^{n-1} \mathbf{A}_j. \quad (20)$$

An important consideration in our design is the selection of a suitable step size τ . A suitable step size τ guarantees the convergence of the design. In order to achieve that, τ should be obtained such that it satisfies the Armijo-Wolfe conditions [9] as follows.

$$f(\mathbf{Y}(\tau)) \leq f(\mathbf{Y}(0)) + \rho_1 \tau f'_{\tau}(\mathbf{Y}(0)) \quad (21)$$

$$f'_{\tau}(\mathbf{Y}(\tau)) \geq \rho_2 f'_{\tau}(\mathbf{Y}(0)), \quad (22)$$

where f'_{τ} is the derivative of f w.r.t. τ and $0 \leq \rho_1 \leq \rho_2 \leq 1$.

$$\begin{aligned} f'_{\tau}(\mathbf{Y}(\tau)) &= \text{Tr} \left(\left(\frac{df}{d\mathbf{Y}(\tau)} \right)^{\mathcal{H}} \mathbf{Y}'(\tau) \right) \\ &= \text{Tr} \left(\mathbf{G}_{\mathbf{Y}(\tau)}^{\mathcal{H}} \mathbf{Y}'(\tau) \right), \end{aligned} \quad (23)$$

and from (14) it can be shown that

$$\mathbf{Y}'(\tau) = - \left(\mathbf{I} + \frac{\tau}{2} \mathbf{S} \right)^{-1} \mathbf{S} \left(\frac{\mathbf{A} + \mathbf{Y}(\tau)}{2} \right). \quad (24)$$

Also from (23), we have

$$f'_{\tau}(\mathbf{Y}(0)) = - \text{Tr}(\mathbf{G}_{\mathbf{A}}^{\mathcal{H}} \mathbf{S} \mathbf{A}). \quad (25)$$

The optimization algorithm can be described as follows.

Algorithm 1 Gradient Descent Algorithm with curvilinear search

- 1: Given an initial point $\mathbf{A}_o \in \mathbb{U}_M$
 - 2: Initialization: Set $k \leftarrow 0$, $\epsilon \geq 0$ and $0 \leq \rho_1 \leq \rho_2 \leq 1$
 - 3: **while** true **do**
 - 4: Prepare: Generate \mathbf{S} .
 - 5: Compute the step size τ_k : Call line search along the path $\mathbf{Y}_k(\tau)$ to obtain a step size τ_k that satisfies the Armijo-Wolfe conditions.
 - 6: Update: $\mathbf{A}_{k+1} \leftarrow \mathbf{Y}(\tau_k)$
 - 7: Stopping Check:
 - 8: **if** $\|\nabla f_{k+1}\| \leq \epsilon$ **then** stop
 - 9: **else** $k \leftarrow k + 1$ and **continue**
-

B. The Direct Design

In this approach, we address the problem of jointly designing all the $|\mathcal{C}|$ constellation points on the unitary group \mathbb{U}_M . The problem can be formulated as follows.

$$\{\mathbf{A}_r\}_{r=1}^{|\mathcal{C}|} = \arg \min_{\mathbf{A}_r \mathbf{A}_r^{\mathcal{H}} = \mathbf{I}} \left(\log \left(\sum_{i=1}^{|\mathcal{C}|-1} \sum_{j=i+1}^{|\mathcal{C}|} e^{\text{Tr}^n(\Re(\mathbf{A}_j^{\mathcal{H}} \mathbf{A}_i))} \right) \right)^{\frac{1}{n}}. \quad (26)$$

The problem of jointly designing $|\mathcal{C}|$ points on the Unitary group \mathbb{U}_M described in the previous equation is equivalent to

a problem of designing one point $\tilde{\mathbf{A}}$ on the Unitary group $\mathbb{U}_{|\mathcal{C}|M}$ where

$$\tilde{\mathbf{A}} = \text{blkdiag}\{\mathbf{A}_1, \mathbf{A}_2, \dots, \mathbf{A}_{|\mathcal{C}|}\}, \quad (27)$$

where blkdiag is the block diagonal operator.

The problem in (26) can now be written as follows

$$\tilde{\mathbf{A}} = \arg \min_{\tilde{\mathbf{A}} \tilde{\mathbf{A}}^{\mathcal{H}} = \mathbf{I}} \left(\log \left(\sum_{i=1}^{|\mathcal{C}|-1} \sum_{j=i+1}^{|\mathcal{C}|} e^{\tilde{u}_{ij}^n} \right) \right)^{\frac{1}{n}}, \quad (28)$$

where

$$\tilde{u}_{ij} = \text{Tr} \left(\Re \left(\mathbf{I}_M^j \tilde{\mathbf{A}}^{\mathcal{H}} \mathbf{I}_M^j \mathbf{I}_M^i \tilde{\mathbf{A}} \mathbf{I}_M^i \right) \right), \quad (29)$$

and \mathbf{I}_M^i is a $M \times |\mathcal{C}|M$ zero matrix with an $M \times M$ identity matrix in the i^{th} block. The gradient $\tilde{\mathbf{G}}_{\tilde{\mathbf{A}}}$ in this case will be given by

$$\tilde{\mathbf{G}}_{\tilde{\mathbf{A}}} = \frac{\left(\log\left(\sum_{i=1}^{|\mathcal{C}|-1} \sum_{j=i+1}^{|\mathcal{C}|} e^{\tilde{u}_{ij}^n}\right)\right)^{\frac{1}{n}-1}}{\sum_{i=1}^{|\mathcal{C}|-1} \sum_{j=i+1}^{|\mathcal{C}|} e^{\tilde{u}_{ij}^n}} \sum_{i=1}^{|\mathcal{C}|-1} \sum_{j=i+1}^{|\mathcal{C}|} e^{\tilde{u}_{ij}^n} \tilde{u}_{ij}^{n-1} \frac{d\tilde{u}_{ij}}{d\tilde{\mathbf{A}}}. \quad (30)$$

The derivative $\frac{d\tilde{u}_{ij}}{d\tilde{\mathbf{A}}}$ can be calculated to be given by [10]

$$\frac{d\tilde{u}_{ij}}{d\tilde{\mathbf{A}}} = \mathbf{I}_M^{j\mathcal{H}} \mathbf{I}_M^i \tilde{\mathbf{A}} \mathbf{I}_M^{i\mathcal{H}} \mathbf{I}_M^j + \mathbf{I}_M^{i\mathcal{H}} \mathbf{I}_M^j \tilde{\mathbf{A}} \mathbf{I}_M^{j\mathcal{H}} \mathbf{I}_M^i. \quad (31)$$

Finally, knowing $\tilde{\mathbf{G}}_{\tilde{\mathbf{A}}}$, the same gradient descent algorithm described in the previous subsection can be used.

It is worth mentioning that the complex dimensions of the block diagonal matrix $\tilde{\mathbf{A}}$ equal $|\mathcal{C}|M^2/2$ not $|\mathcal{C}|^2M^2/2$ (the complex dimension of the manifold $\mathbb{U}_{|\mathcal{C}|M}$). So, $\tilde{\mathbf{A}}$ belongs to a submanifold of $\mathbb{U}_{|\mathcal{C}|M}$ and this new submanifold is called $\tilde{\mathbb{U}}_{|\mathcal{C}|M}$. We can easily check that the gradient descent algorithm can be used in the direct approach by observing that $\tilde{\mathbf{G}}_{\tilde{\mathbf{A}}}$ is also a block diagonal matrix. This means that if we started from an initial point on $\tilde{\mathbb{U}}_{|\mathcal{C}|M}$, the subsequent trial points will also be in the same submanifold $\tilde{\mathbb{U}}_{|\mathcal{C}|M}$. Hence, the gradient descent algorithm can be used in the case of the direct approach also.

V. SIMULATION RESULTS

In this section, we evaluate the performance of different constellations of unitary codes designed with the greedy approach and the direct approach, and compare their performance with the Alamouti code for 2×2 case and a unitary code constructed based on the Alamouti code for the 4×4 case.

Figure 2 shows the performance curves of 2×2 codes with different constellation sizes (256 points and 1024 points) designed using the gradient descent algorithm over the unitary group \mathbb{U}_2 with both the greedy and direct approaches. These constellations can be used as the HR layer of a MIMO system with two transmit antennas. The designed codes performance is compared with the corresponding performance of 2×2 Alamouti codes such that each sample used in the Alamouti code is drawn from a constant modulus constellation to guarantee the unitarity of the Alamouti code.

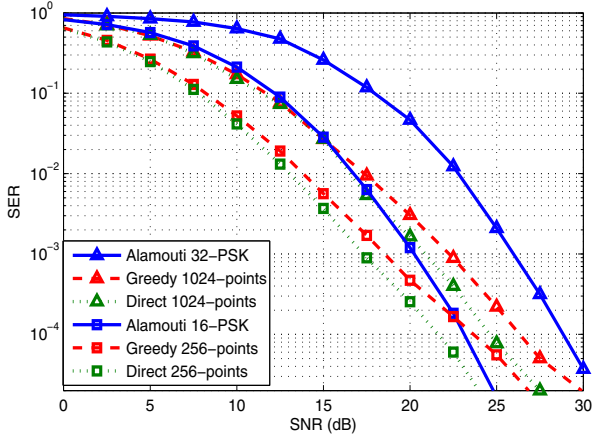


Fig. 2: Comparison between SER of the 256-point and 1024-point 2×2 codes designed over \mathbb{U}_2 using the greedy approach, direct approach and the corresponding, same rate, Alamouti codes.

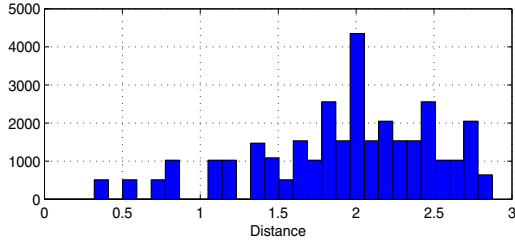


Fig. 3: Histogram of the Frobenius distances for the 256-point 2×2 Alamouti code. ($d_{min} = 0.3902$)

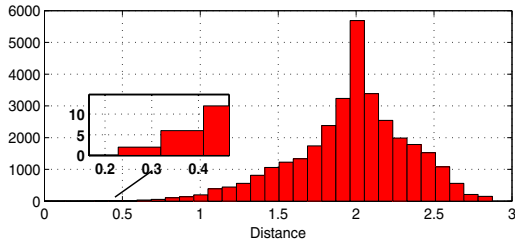


Fig. 4: Histogram of the Frobenius distances for the 256-point HR code designed over \mathbb{U}_2 using the greedy approach. ($d_{min} = 0.2356$)

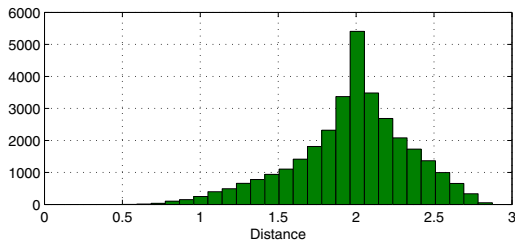


Fig. 5: Histogram of the Frobenius distances for the 256-point HR code designed over \mathbb{U}_2 using the direct approach. ($d_{min} = 0.5641$)

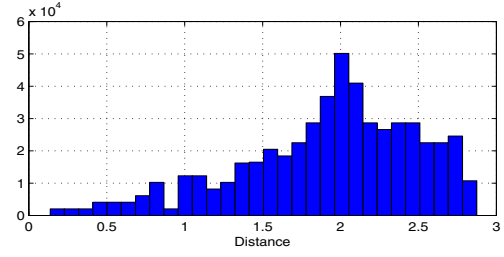


Fig. 6: Histogram of the Frobenius distances for the 1024-point 2×2 Alamouti code. ($d_{min} = 0.196$)

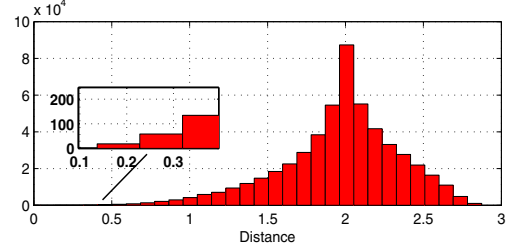


Fig. 7: Histogram of the Frobenius distances for the 1024-point HR code designed over \mathbb{U}_2 using the greedy approach. ($d_{min} = 0.1597$)

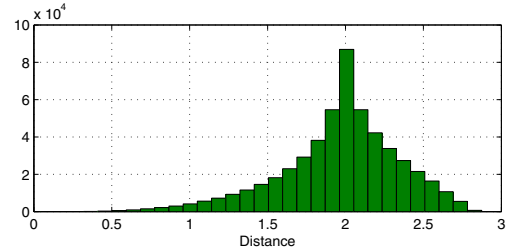


Fig. 8: Histogram of the Frobenius distances for the 1024-point HR code designed over \mathbb{U}_2 using the direct approach. ($d_{min} = 0.3209$)

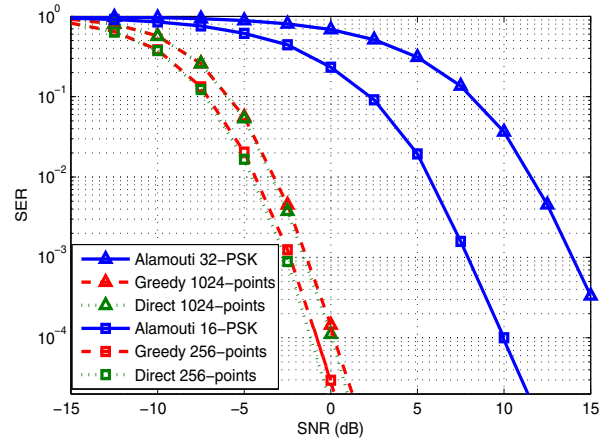


Fig. 9: Comparison between SER of the 256-point and 1024-point 4×4 codes designed over \mathbb{U}_4 using the greedy approach, direct approach and the corresponding, same rate, Alamouti-based codes.

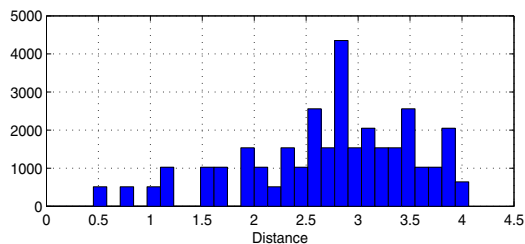


Fig. 10: Histogram of the Frobenius distances for the 256-point 4×4 Alamouti-based code. ($d_{min} = 0.5518$)

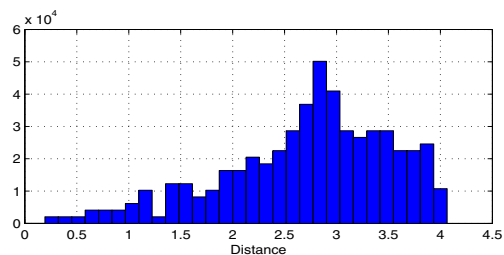


Fig. 13: Histogram of the Frobenius distances for the 1024-point 4×4 Alamouti-based code. ($d_{min} = 0.2772$)

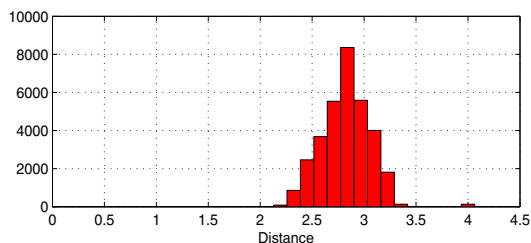


Fig. 11: Histogram of the Frobenius distances for the 256-point HR code designed over \mathbb{U}_4 using the greedy approach. ($d_{min} = 2.1811$)

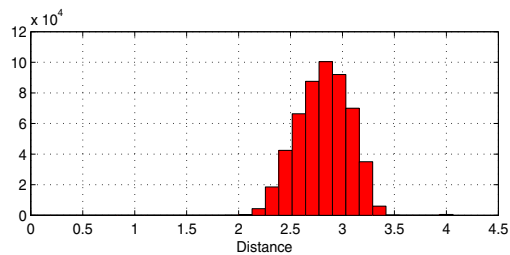


Fig. 14: Histogram of the Frobenius distances for the 1024-point HR code designed over \mathbb{U}_4 using the greedy approach. ($d_{min} = 1.9907$)

Figures 3, 4 and 5 show the histogram of the Frobenius distances for the 256-point 2×2 Alamouti, greedy and direct codes, respectively. It is noted that the minimum Frobenius distance in case of the Alamouti code ($d_{min} = 0.3902$) is higher than the minimum Frobenius distance in case of the greedy code ($d_{min} = 0.2356$), which explains why the Alamouti code is superior at high SNRs. However, it is clear from the same histograms in Figures 3 and 4 that the intensity of low distances is higher in the Alamouti code histogram than the greedy code histogram, which explains why the Alamouti code is worse than the designed code in channels with high noise power. For the direct code, we can see from the histogram in Figure 5 that the minimum distance is 0.5641 which is higher than the minimum distance of the Alamouti code.

The same previous behaviour, but for the 1024-point codes, is shown in Figures 6, 7 and 8 which show the histogram of the Frobenius distances for the 1024-point 2×2 Alamouti, greedy and direct codes, respectively.

Figure 9 shows the performance curves of 4×4 codes with different constellation sizes (256 points and 1024 points) designed using the gradient descent algorithm over the unitary group \mathbb{U}_4 with both the greedy and direct approaches. These unitary codes can be used as the HR layer of a MIMO system with four transmit antennas, compared with performance curves of the corresponding, same rate, 4×4 unitary codes constructed based on the Alamouti scheme as follows:

$$\mathbf{A} = \frac{1}{\sqrt{2}} \begin{pmatrix} \hat{\mathbf{A}} & \hat{\mathbf{A}} \\ -\hat{\mathbf{A}} & \hat{\mathbf{A}} \end{pmatrix}, \quad (32)$$

where

$$\hat{\mathbf{A}} = \frac{1}{\sqrt{2}} \begin{pmatrix} s_1 & s_2 \\ -s_2^* & s_1^* \end{pmatrix}, \quad (33)$$

where s_1 and s_2 are two complex symbols drawn from any constant modulus constellation, e.g., PSK.

From Figure 9 we can see that the designed codes are always better than the corresponding ‘‘Alamouti-based’’ codes. For example, it is clear in this figure that the greedy 256-point 4×4 code is superior to the 4×4 Alamouti-based code

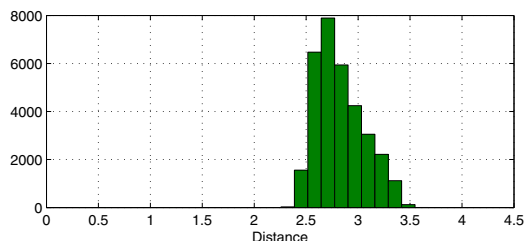


Fig. 12: Histogram of the Frobenius distances for the 256-point HR code designed over \mathbb{U}_4 using the direct approach. ($d_{min} = 2.3421$)

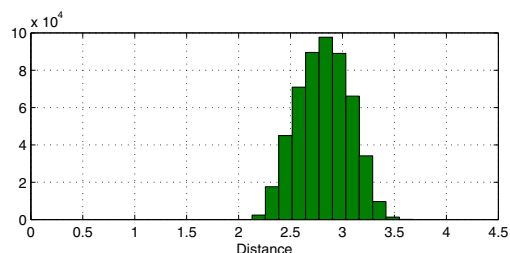


Fig. 15: Histogram of the Frobenius distances for the 1024-point HR code designed over \mathbb{U}_4 using the direct approach. ($d_{min} = 2.0576$)

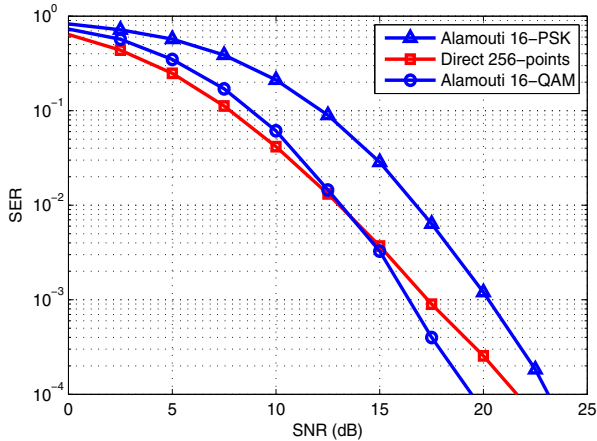


Fig. 16: Comparison between SER of 16-PSK, 16-QAM Alamouti 2×2 schemes and the 256-point 2×2 codes designed over \mathbb{U}_2 using the direct approach.

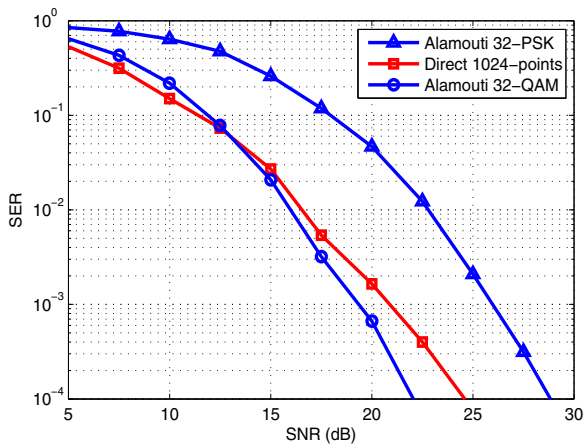


Fig. 17: Comparison between SER of 32-PSK, 32-QAM Alamouti 2×2 schemes and the 1024-point 2×2 codes designed over \mathbb{U}_2 using the direct approach.

by about 10 dB at a SER of 10^{-4} . Note that this Alamouti-based code has the same rate as the designed codes (2 bits per channel use) and constructed using 2 symbols, each of them is carved from the 16-PSK constellation. Finally, it is shown in the same figure that the performance of the greedy 1024-point 4×4 code is better than the 4×4 Alamouti code - that has the same rate as the designed codes (2.5 bpcu) and constructed using 2 symbols each of them is carved from the 32-PSK constellation - by 15 dB.

Figures 10, 11 and 12 show the histogram of the Frobenius distances for the 256-point 4×4 Alamouti-based, greedy and direct codes, respectively, while Figures 13, 14 and 15 show the histogram of the Frobenius distances for the 1024-point 4×4 Alamouti-based, greedy and direct codes, respectively.

Finally, Figure 16 compares the SER performance of 16-PSK, 16-QAM Alamouti 2×2 schemes and the 256-point 2×2 codes designed over \mathbb{U}_2 using the direct approach and Figure 17 compares between 32-PSK, 32-QAM Alamouti 2×2

schemes and the 1024-point 2×2 codes designed over \mathbb{U}_2 using the direct approach. It is clear from these figures that the 256-point and 1024-point 2×2 direct codes are superior to the 16-QAM and 32-QAM Alamouti codes in low and medium SNRs up to 12.5 dB. Therefore, the proposed codes can still achieve better than the conventional space-time code (which are not unitarily-constrained).

VI. CONCLUSION

In this paper, we propose new unitary space-time block codes designed using the gradient descent algorithm over Stiefel manifold with two different approaches: the greedy approach in which the constellation points are designed in a point-by-point manner and the direct approach in which all the constellation points are jointly designed. The designed codes are shown to outperform the unitarily-constrained conventional space-time block codes; they are also shown to outperform some non-unitarily constrained space-time block codes at low and medium SNRs. These designed unitary codes can be used as the high resolution codes for any arbitrary number of transmit antennas M in a layered coding settings.

REFERENCES

- [1] M.T. Hussien, K.G. Seddik, R.H. Gohary, M. Shaqfeh, H. Alnuweiri, and H. Yanikomeroglu, "Multi-resolution broadcasting over the grassmann and stiefel manifolds," in *2014 IEEE International Symposium on Information Theory (ISIT)*, June 2014, pp. 1907–1911.
- [2] Yang Li and A. Nosratinia, "Grassmannian-euclidean superposition for mimo broadcast channels," in *2012 IEEE International Symposium on Information Theory Proceedings (ISIT)*, July 2012, pp. 2491–2495.
- [3] Yang Li and A. Nosratinia, "Product superposition for mimo broadcast channels," *IEEE Transactions on Information Theory*, vol. 58, no. 11, pp. 6839–6852, Nov 2012.
- [4] Lihong Zheng and D.N.C. Tse, "Communication on the grassmann manifold: a geometric approach to the noncoherent multiple-antenna channel," *IEEE Transactions on Information Theory*, vol. 48, no. 2, pp. 359–383, 2002.
- [5] R.H. Gohary and T.N. Davidson, "Noncoherent mimo communication: Grassmannian constellations and efficient detection," *IEEE Transactions on Information Theory*, vol. 55, no. 3, pp. 1176–1205, March 2009.
- [6] I. Kammoun, A.M. Cipriano, and J.C. Belfiore, "Non-coherent codes over the Grassmannian," *IEEE Transactions on Wireless Communications*, vol. 6, no. 10, pp. 3657–3667, 2007.
- [7] S. M. Alamouti, "A simple transmit diversity technique for wireless communications," *IEEE Journ. Sel. Areas in Comm.*, vol. 16, no. 8, pp. 1451–1458, Oct. 1998.
- [8] Zaiwen Wen and Wotao Yin, "A feasible method for optimization with orthogonality constraints," in *In Rice Univ. Technical Report 10. 4*.
- [9] "Line search methods," in *Numerical Optimization*, Springer Series in Operations Research and Financial Engineering, pp. 30–65. Springer New York, 2006.
- [10] Kaare Brandt Petersen, Michael Syskind Pedersen, Jan Larsen, Korbinian Strimmer, Lars Christiansen, Kai Hansen, Liguang He, Loic Thibaut, Miguel Baro, Stephan Hattinger, Vasile Sima, and We The, "The matrix cookbook," Tech. Rep., 2006.